Robotica (2009) volume 27, pp. 379–387. © 2008 Cambridge University Press
doi:10.1017/S0263574708004797 Printed in the United Kingdom

Design of series damper actuator

Wei Zhou, Chee-Meng Chew* and Geok-Soon Hong

Department of Mechanical Engineering, National University of Singapore, Singapore 119260

(Received in Final Form: June 2, 2008. First published online: July 4, 2008)

SUMMARY
In our previous work, a novel force control actuator, called series damper actuator (SDA), has been proposed. This paper proposes a general design procedure for the SDA system. From design requirements, several key parameters of the SDA plant can be determined. Based on these parameters, the selection or design of the series damper and the motor can be carried out. A case study is included to illustrate the effectiveness of the procedure. As there could be more than one feasible solutions from the procedure, the mechatronic design quotient (MDQ) method can be adopted to select the best solution from a feasible solution space.

KEYWORDS: Force control actuators; Series damper actuators; Plant design; Design optimization; Mechatronic design quotient.

1. Introduction

Force control is very important for robots, especially for those that need to interact with unknown environments or human, such as assembly manipulators, legged robots, haptic devices, and tele-operation systems. Force control actuators have been widely used to achieve low impedance and human friendly actuation for robots.[1–4] Pratt has proposed a type of force control actuator, called series elastic actuator (SEA).[5–7] The key feature of this actuator is the presence of a series elastic component between the motor and the load. The actuator's output force is achieved by controlling the deformation of the elastic component (assume that its elastic property is known).

In our recent work, a novel force control actuator called series damper actuator (SDA) has been proposed.[8,9] Having a similar topology as that of the SEA system, the SDA system uses a damper as the series component. The actuator output force can be indirectly controlled by controlling the damper's relative velocity, given the constitutive property of the damper. The advantages of the SDA system include high force fidelity, large bandwidth, high impact tolerance ability, and large output range.

In our previous work, the SDA system has been modeled and analyzed in detail. The controller design has also been investigated. In our patent application file,[10] a rough hardware design of the SDA system, including the system architecture, the mechanical structure, etc., has been presented. However, the selection process for the series damper and the DC motor was not specified. Since a proper selection of the series damper and the motor is necessary to ensure successful design of a SDA system, we need to devise a systematic approach for the selection process. This paper aims to provide a systematic design procedure for the SDA system especially in terms of the series damper and motor selection. Given the system performance requirements or parameters, the various design parameters can be generated. These parameters enable the designer to design or select appropriate components for the system. In Section 2, the SDA system is introduced and a general plant structure is also presented. In Section 3, the selection/design steps for the damper and the motor are introduced. In Section 4, the best motor is selected based on the mechatronic design quotient (MDQ) method. Conclusions and comments are presented at the end of this paper.

2. Series Damper Actuator

The SDA system incorporates a series damper instead of a series elastic element between the driving actuator and the load. The block diagram of a SDA system with motor being the driving actuator is shown in Fig. 1. Such SDA system typically has a control module and the following hardware modules: a motor with appropriate gear transmission and a damper. The system is designed to effectively control the relative velocity in the damper to achieve the desired force (given the damping coefficient of the damper). The damper is assumed to be viscous and the damping force can be expressed as follows:

$$f = B v_D \tag{1}$$

where B is the damping coefficient and v_D is the relative velocity between the input and output shafts of the damper.

System analysis has been done[8] and it is shown that SDA system has high force fidelity, large output range, large system bandwidth, low output impedance, high impact tolerance ability, etc. The SDA system uses a damper as the series component and its system order is lower than that of the SEA system. Hence, in general, SDA processes a larger bandwidth compared to the latter.

Another advantage of SDA is that the damping coefficient of the damper can be made variable by adopting an appropriate damper design. For example, one possible design is to adopt magneto-rheological (MR) fluid, which has variable rheological property. The damping coefficient can become a controlled variable, which can be adjusted according to the environmental conditions.

For example, when high force and low force outputs are required, the damping coefficient can be increased and

*Corresponding author. E-mail: chewcm@alum.mit.edu

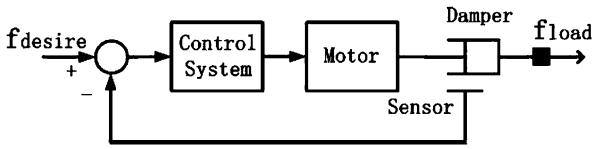

Fig. 1. Schematic diagram of series damper actuator.

reduced, respectively, to yield corresponding feasible relative velocity in the damper. This endows the system with higher force fidelity at both high and low force range.

Furthermore, the series damper actuator has a distinctive advantage of impact absorption due to the damper energy dissipation characteristic. This characteristic is very important for walking robots, haptic devices, or robot manipulators to protect them from damage when they are subjected to external impact. However, the dissipative characteristic results in lower energy efficiency for SDA as compared to SEA.

The design of the SDA plant involves the determination of the target design parameters followed by the selection of the appropriate hardware modules: the motor (with gear reduction) and the series damper. For the hardware selection, the designer needs to consider a number of important issues. For example, in selecting the motor, the bandwidth, the maximum power, and the suitable gear reduction, should be considered. As for the series damper, the range of the variable damping coefficient, the bandwidth (if any), etc. should be considered. The overall bandwidth of the plant should also be checked. In this paper, a general design procedure which incorporates these design considerations is introduced.

3. Component Selection for SDA System

In general, the SDA plant includes a series damper, a motor, sensors, a motor driver, and a microcontroller. The SDA hardware design should begin with the selection or design of the series damper and the motor. It is because the selection of the other hardware components, such as the sensors and the motor driver, is usually dependent on the selected damper and motor. Between the damper and the motor, the former should be considered first, since the choices of the damper are quite limited, while there are more choices for the motor.

The following are the key parameters from the design specifications: (a) Maximum output force F_{L_max}; (b) Maximum load velocity V_{L_max}; and (c) Minimum system bandwidth ω_{min}. In the following subsections, these parameters will be used to generate the design parameters for the damper and the motor.

3.1. Damper selection

The series damper in the SDA system can either be linear or rotary. The choice depends on whether the SDA system is meant to deliver linear force or torque. There are also several approaches to achieve the damping effect. The common damper types include viscous damper, MR fluid damper, electro-rheological (ER) fluid damper, eddy current damper, powder clutch, etc.

The considerations for the damper may include the output force, operating speed, damping coefficient, bandwidth, size, weight, cost, etc. For the initial design consideration, the operating speed, the damping coefficient, and the bandwidth are considered.

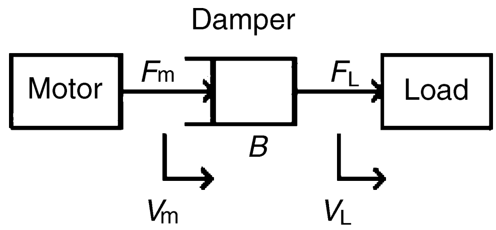

Fig. 2. General model of SDA actuator plant.

Since the series damper is required to have a variable damping coefficient, it is important to specify the desired range of its damping coefficient. The minimum damping coefficient is desirable to be as low as possible so that the system can achieve good low force performance. For the initial design purpose, the maximum damping coefficient B_{max}, the maximum damper relative velocity V_{D_max}, and the minimum damper bandwidht ω_D should be determined as shown in the following steps.

Step 1. Maximum variable damping coefficient B_{max}.

The maximum damping coefficient B_{max} can be determined by considering the desired efficiency for the damper. The general model of the SDA plant, consisting of a damper serially connected between the motor and the load, is shown in Fig. 2, where f_m is the motor output force, v_m is the motor output velocity, f_L is the actuator output force (load force), v_L is the actuator output velocity (load velocity), and B is the damping coefficient. When the SDA actuator system operates under active mode, power will be transmitted from the motor to the load through the series damper. The input and output power for the damper can be expressed as follows:

Damper input power p_m:

$$p_m = f_m \cdot v_m. \tag{2}$$

Damper output power p_L:

$$p_L = f_L \cdot v_L. \tag{3}$$

Neglecting the inertia force of the damper, we have

$$f_m = f_L \tag{4}$$

and from Eq. (1)

$$f_L = B v_D = B(v_m - v_L) \tag{5}$$

where $v_D = v_m - v_L$ is the damper's relative velocity.

From Eq. (5), v_m can be expressed as follows:

$$v_m = \frac{f_L}{B} + v_L. \tag{6}$$

https://doi.org/10.1017/S0263574708004797 Published online by Cambridge University Press

Therefore, the efficiency η for the power transmitted through the series damper is

$$\eta = \frac{p_L}{p_m} = \frac{v_L}{v_m} = \frac{v_L}{\frac{f_L}{B} + v_L}. \tag{7}$$

From Eq. (7), B can be expressed as follows:

$$B = \frac{\eta f_L}{(1-\eta) v_L}. \tag{8}$$

In the SDA system, the maximum damping coefficient B_{max} typically corresponds to the maximum output force F_{L_max}. And let us assume that when the actuator is generating the maximum output force, the system is required to have a certain efficiency η_m $(0 < \eta_m < 1)$ at the maximum load velocity V_{L_max}. The maximum damping coefficient B_{max} can then be computed using the above conditions as follows:

$$B_{max} = \frac{\eta_m F_{L\_max}}{(1-\eta_{max}) V_{L\_max}}. \tag{9}$$

Step 2. Maximum damper relative velocity V_{D_max}.

The maximum damper relative velocity V_{D_max} is assumed to be corresponding to the maximum output force F_{L_max}. Let us also assume that the corresponding damping coefficient is at the maximum value. The maximum damper's relative velocity V_{D_max} is

$$V_{D\_max} = \frac{F_{L\_max}}{B_{max}}. \tag{10}$$

Step 3. Minimum damper bandwidth ω_D.

With the damper relative velocity v_D as the input and the damping force f_L as the output, the series damper has a transfer function as follows:

$$G_D(s) = \frac{F_L(s)}{V_D(s)}. \tag{11}$$

The bandwidth is the frequency, at which the system frequency response (gain) has declined by 3 dB from its low-frequency value.[11]

For a linear viscous damper whose constitutive equation can be expressed as in Eq. (1)

$$f_L = B v_D \tag{12}$$

where B is the constant damping coefficient. Therefore, the transfer function for such a viscous damper is

$$G_D(s) = \frac{F_L(s)}{V_D(s)} = B. \tag{13}$$

Since it is a zero-order system, the bandwidth is infinite. However, this may not be true for some types of dampers such as the MR fluid damper. To emulate a viscous damper defined in Eq. (12), the MR fluid damper is controlled by a linearization algorithm to produce damping coefficient B. [9] This linearization process introduces some extra dynamics into the series damper, such as the electromagnetic response of the MR fluid. Therefore, the bandwidth of such virtual viscous damper is lower than that of a real viscous damper.

To consider the bandwidth property of the virtual viscous damper, a first-order model was used to represent the damper dynamics [9]:

$$G_D(s) = \frac{F_L(s)}{V_D(s)} = B\frac{\omega_D}{s + \omega_D}. \tag{14}$$

where ω_D is the high cut-off frequency or the bandwidth. In this case, the bandwidth of the series damper should be large enough so that the overall bandwidth of the SDA plant can be achieved.

Statement 1: To ensure a minimum overall bandwidth ω_{min} for the SDA plant, the damper's bandwidth should satisfy the following requirement:

$$\omega_D \geq \frac{1}{0.64}\omega_{min}. \tag{15}$$

The proof of Statement 1 is included in Appendix A. Equation (15) defines the minimum damper bandwidth for the SDA system to achieve a certain overall bandwidth. The damper bandwidth can be experimentally measured using the frequency response method to ensure that it satisfies the minimum requirement.

Now, the damper can be designed or chosen so that the above three criteria, damping coefficient range, maximum relative velocity, and minimum bandwidth, are fulfilled. Furthermore, the other requirements such as size, weight, and cost, if any, should also be satisfied. The damper's heat dissipation issue should also be considered especially if the force-to-size ratio is quite high. Heat sink can be added, if necessary.

3.2. Motor selection

A motor should be selected to match the damper selected in the previous subsection. Let us assume that permanent magnet DC motors are considered for the SDA system. For such a motor, considerations must be given to the power, speed, torque, bandwidth, size, weight, etc. A suitable gear transmission device (harmonic drive, lead screw, etc.) may have to be chosen as well, depending on the application. The following are the steps used to select a suitable DC motor based on the design requirements and selected series damper.

Step 1. Maximum motor output velocity V_{m_max}.

The maximum motor output velocity V_{m_max} (after the gear reduction, if any) can be calculated as follows:

$$V_{m\_max} = (1+\alpha)(V_{D\_max} + V_{L\_max}). \tag{16}$$

where α $(0 < \alpha < 1)$ is a constant value to provide some safety margin.

Step 2. Output power of motor P_m.

If the efficiency of the gear transmission is assumed to be 100% and the damper's inertia force is negligible, the motor's

https://doi.org/10.1017/S0263574708004797 Published online by Cambridge University Press

output force f_m is equal to the actuator's output force (load force) f_L. Hence, the required motor's output power can be computed as follows:

$$P_m = F_{L\_max} \cdot V_{m\_max}. \tag{17}$$

Step 3. Selecting a motor based on the power requirement.

Here, we choose a motor which can deliver the required output power. For motor efficiency consideration, the chosen motor should have a maximum power roughly twice the power requirement computed in the previous step.

Step 4. Gear reduction N.

After the motor is selected, the following motor parameters can be obtained from the motor specifications: the maximum rotor output torque M_{e_max} and the maximum rotor speed n_{e_max}. These quantities will be used to determine the required gear reduction.

The minimum gear ratio should be calculated based on the required maximum motor's output torque F_{L_max}

$$N_{min} = \frac{F_{L\_max}}{M_{e\_max}} \tag{18}$$

while the maximum gear ratio can be calculated based on the required maximum motor's output speed V_{m_max}

$$N_{max} = \frac{n_{e\_max}}{V_{m\_max}}. \tag{19}$$

We have to check and ensure that the calculated N_{max} should be larger than N_{min}. If this is not true, the motor selected is not suitable and an alternative motor should be sourced (go back to Step 3). Otherwise, the suitable gear reduction should be between N_{min} and N_{max}.

After the gearhead is selected, the efficiency problem should be first checked to ensure that the output torque still meets the design requirement by fulfilling following relationship:

$$M_{e\_max} \cdot N \cdot \eta_g \geq F_{L\_max} \tag{20}$$

where N is the gear reduction and η_g is the efficiency of the selected gearhead. If this not satisfied, the gearhead should be changed, or we need to go back to Step 3 to select another suitable motor.

Step 5. Motor's bandwidth $\omega_{m'}$.

The motor's open loop (voltage input and velocity output) bandwidth should be larger than the required value.

Statement 2: To ensure a minimum overall bandwidth ω_{min} for the SDA plant, the DC motor (free end) bandwidth $\omega_{m'}$ should satisfy the following requirement:

$$\omega_{m'} \geq \frac{J_m + J_D/N^2}{0.64 J_m}\omega_{min} \tag{21}$$

where J_m is the motor's inertia and J_D is the damper's input-end inertia.

The proof of Statement 2 is included in Appendix B. Equation (21) defines the minimal bandwidth requirement of the DC motor. After the motor is selected, the motor bandwidth should be tested. If Eq. (21) cannot be satisfied, the motor and/or the gearhead should be changed.

Step 6. Motor rotor inertia J_m.

In the SDA system, the load is separated from the motor by the series damper. The output shaft of the motor is connected to the input end of the series damper. Therefore, for the consideration of the inertia matching, the motor rotor inertia J_m should not be too small compared to the damper's input-end inertia J_D. If a gear reduction N is used to increase the motor's output torque, the damper's input-end inertia reflected onto the motor shaft will be reduced to J_D/N^2. For most cases, the reflected input-end inertia of damper J_D/N^2 is much smaller than the motor rotor inertia J_m. If it is not true, a larger gear reduction or a motor with a larger rotor inertia should be used.

Step 7. Required maximum motor torque F_{m_max}.

Neglecting the inertia and the frictional effect, the required motor torque is given by

$$F_{m\_max} = \frac{F_{L\_max}}{N}. \tag{22}$$

Check and ensure that $F_{m\_max} \leq M_{e\_max}$. Otherwise, go back to Step 3 to change the selected motor.

Step 8. Required motor current I_{max}.

The motor current I_{max} required to generate the maximum motor torque F_{m_max} is given by

$$I_{max} = \frac{F_{m\_max}}{k_m} \tag{23}$$

where k_m is the torque constant of the motor.

Check and ensure that I_{max} is smaller than the motor-rated current. Otherwise, go back to Step 3 to change the selected motor.

Here, we have described how to select a suitable damper and motor for the SDA system. The design procedure may need several iterations before a satisfied plant can be achieved. Furthermore, the SDA plant component design/selection steps described above are dependent on the design specifications. Different initial design specifications or requirements may result in different design considerations and, consequently, different design steps. But the general steps described above can provide the basic idea and serve as a guideline on how to design the SDA plant. They also allow the designer to proceed to identify some specific design cases.

4. Case Study

An example of the SDA plant design is discussed in this section. The initial design specifications are given in Table I.

Table I. Specifications for SDA plant design.

Actuator type	Rotary
Maximum output force (F_{L_max})	3 Nm
Maximum load velocity (V_{L_max})	4 rad/s
Minimum system bandwidth (ω_{min})	7 Hz
Across damper power efficiency (η_m)	0.5
Motor velocity margin factor (α)	50%

https://doi.org/10.1017/S0263574708004797 Published online by Cambridge University Press

Table II. Typical data of MRB-2107-3 MR brake.

Maximum torque	5.6 Nm
Damping coefficient varying range (virtual)	$0 \sim \infty$ Nms (theoretically)
Bandwidth	25 Hz
Maximum operating speed	1000 rpm (105 rad/s)
Input end inertia (J_D)	1600 gcm^2
Diameter	92.2 mm
Length	36.6 mm
Weight	1410 g
Operating temperature range	−30°C to 70°C

Table III. Specifications of two suitable DC motor solutions.

	Motor Solution 1 (Faulbaber 4490H024B)	Motor Solution 2 (Faulbaber 3863A024C)
Nominal voltage	24 V	24 V
Output power	201 W	220 W
Weight (excluding gear box)	750 g	400 g
Rotor inertia (J_m)	130 gcm^2	110 gcm^2
Speed up to	16,000 rpm	8000 rpm
Torque up to	191.8 mNm	110 mNm
Current up to	8.62 A	3.8 A
Gear reduction (N)	23	43
Gear reduction efficiency (η_g)	0.8	0.7

Following the design steps described in the last section, an MR brake (MRB-2107-3, Lord Corporation) and a DC permanent magnet motor (3863A024C, Faulhaber) are chosen as the series damper and the motor, respectively, for the SDA system. The specifications of the selected MR fluid damper (MRB-2107-3) and the DC motor (3863A024C) are shown in Tables II and III, respectively. A setup of the designed SDA system was built which is shown in Fig. 3. In this setup, besides the motor and the series damper, there are two encoders mounted to measure the damper's input and output velocities, respectively. The relative velocity of the damper is obtained from the difference between the velocity readings from these two encoders. This SDA system has also been tested and shown to achieve satisfied results as reported in refs. [8, 9].

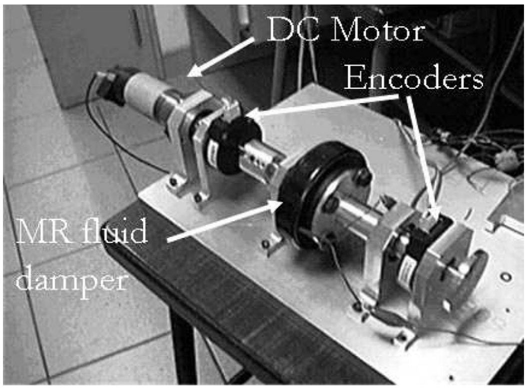

Fig. 3. Photograph of the designed series damper actuator plant.

The suitable motor is selected by using the previous procedures. Since there are many motors from different companies with different types, parameters, performances, and costs, the choice is typically not unique. For example, besides the mentioned Faulbaber 3863A024C (Motor Solution 2), another motor Faulhaber 4490H024B (Motor Solution 1) is also a suitable solution for the design requirements as shown in Table III. Since the choice is not unique, we need to establish a systematic approach to identify the "best" choice. In the next section, a design optimization tool is used for such a purpose.

5. Design Optimization Using Mechatronic Design Quotient

As mechatronic system design typically involves many issues, the process can be very complex. In this section, the mechatronic design quotient proposed by de Silva [12,13] is applied to choose an optimal design from a set of feasible solutions. For illustration purpose, it is applied to select the best motor from a given set of feasible choices for our SDA design. An MDQ approach typically includes the following steps:[14]

1. Identify the relevant MDQ issues including the understanding of the design goals; identifying the basic performance, tasks, and requirements for the desired system; and figuring out what issues come under multiple design criteria.
2. Establish the MDQ aspects and quantify the requirements. In this step, one should identify those criteria that are considered to be very important in the design, such as cost, reliability, bandwidth, weight, and size. After establishing the MDQ aspects, the pertinent requirements have to be quantified, and a table of target specifications should be formed.
3. Establish a database for feasible designs. This step identifies design solutions which would roughly satisfy the basic performance requirements. All feasible solutions together form a feasible solution space.
4. Assign MDQ indices I_i's to each feasible solution. For each MDQ aspect, there will be a corresponding design index I_i for each solution. It is a measure of the degree to which a particular design solution satisfies a design aspect. Each MDQ index also includes a weighting factor which indicates the importance of that particular aspect in the overall design.
5. Compute the aggregate MDQ index. In this step, one incorporates all individual design indices and associated weighting factor to obtain the value of the overall MDQ index. A final decision is made by selecting the design with the highest MDQ value.

Following the steps described above, we apply the MDQ for the motor selection. The motor selection for the SDA system can be rather a complex issue. The key design criteria used are size, weight, cost, bandwidth, and speed. The MDQ procedure is illustrated in Fig. 4. The target specifications have been quantified and tabulated in Table IV.

The next step is to find the information of available commercial products and establish a database for the feasible solution space. Selecting suitable motors for the solution

https://doi.org/10.1017/S0263574708004797 Published online by Cambridge University Press

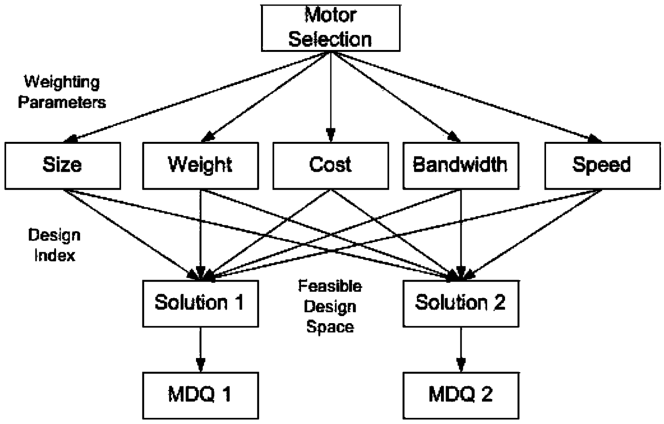

Fig. 4. MDQ applied to the motor selection.

Table IV. Target specifications for motor selection.

Maximum size	ø50 mm × 200 mm
Maximum weight	1000 g
Maximum cost	S$ 800
Minimum bandwidth	11 Hz
Minimum speed	6000 rpm

space should follow the steps described in the previous section. For illustration purpose, only two suitable motor candidates are identified and included in the feasible solution space. The two suitable motors are Faulhaber 3863A024C and 4490H024B as mentioned before. Then the solution space with the various MDA aspects is shown in Table V.

These candidate solutions satisfy the five requirements (MDQ aspects) to different extents. We assign one index I_{mn} to each MDQ aspect to indicate the degree to which a particular solution satisfies it. m is an integer number from 1 to 5 representing these five MDQ aspects. n is an integer number of 1 or 2 representing the two candidate motors of the solution space. Furthermore, a weighting factor W_m is assigned for each MDQ aspect. In this case, we assign $W_1 = 25\%$, $W_2 = 25\%$, $W_3 = 20\%$, $W_4 = 15\%$, and $W_5 = 15\%$ to indicate that the size and the weight are the most important attributes, while the bandwidth and the speed are the less important attributes. The weighting factors sum up to 100%.

The MDQ indices are assigned as shown in Table VI. It is important to make sure that the relative performance of each solution across each aspect is properly reflected by the relative magnitudes of the indices. To compute the aggregate MDQ index M_j for solution j, simply incorporate all the design indices and weighting factors according to the

Table V. Solution database.

MDQ aspects	Solution 1	Solution 2
Size	ø44 mm × 168 mm	ø38 mm × 107 mm
Weight	750 g	400 g
Cost	S$584	S$434
Bandwidth	20 Hz	13 Hz
Speed	16,000 rpm	10,000 rpm

Table VI. MDQ indices values.

Design index	Solution 1 (%)	Solution 2 (%)	Maximum value I_{im} (%)	Weighting parameter (%)
Size index (I_1)	50	80	80	25
Weight index (I_2)	40	80	80	25
Cost index (I_3)	60	80	80	20
Bandwidth index (I_4)	80	65	80	15
Speed index (I_5)	80	50	80	15
MDQ value (M)	73.13	91.56	N.A.	N.A.

following equation:

$$M_j = \frac{\sum_{i=1}^{5} W_i I_{ij}}{\sum_{i=1}^{5} W_i I_{im}}. \quad (24)$$

Note that $0 < M_j \leq 100\%$. The results of the calculated M_j are shown in the last row of Table VI.

The last step is to select the solution with the highest MDQ value to be the best choice. Therefore, the second solution, that is Faulhaber 3863A024C, is the best choice between the two feasible motor solutions.

6. Conclusion

In this paper, a general design procedure for the SDA plant has been presented. The procedure allows us to determine, with given design requirements, the key parameters of the SDA plant, such as the damping coefficient range, component bandwidth, motor power, and gear ratio. Thereafter, the series damper and motor can be selected or designed accordingly. Based on these procedures, an experimental SDA system has been successfully developed in the case study.

Note that it is impossible to devise a universal design procedure for the SDA system. Different design cases may have different requirements and initial conditions which require different design procedures. Nevertheless, the design procedures described in this paper can provide some basic guidelines for the general SDA system design.

This paper also illustrated the use of the MDQ method to identify the best choice of motors among a given feasible solution set. In MDQ, the relative suitability of the candidate solutions can be easily quantified. In fact, the application of MDQ can be extended to the design of the whole SDA system, rather than the motor selection only.

Acknowledgment

This project is funded by the Academic Research Fund of the National University of Singapore.

References

1. N. Takesue, H. Asaoka, J. Lin, M. Sakaguchi, G. Zhang and J. Furusho, "Development and Experiments of Actuator Using MR Fluid," *IEEE International Conference on Industrial Electronics, Control and Instrumentation*, Nagoya, Japan (2000) pp. 1838–1843.

https://doi.org/10.1017/S0263574708004797 Published online by Cambridge University Press

2. G. A. Pratt, C. Bolton, P. Willisson and A. Hofman, "Late Motor Processing in Low-Impedance Robots: Impedance Control of Series-Elastic Actuators," *American Control Conference*, vol. 4, Boston, MA (2004) pp. 3245–3251.
3. J. S. Sulzer, M. A. Peshkin and J. L. Patton, "Marionet: An Exotendon-Driven Rotary Series Elastic Actuator for Exerting Joint Torque," *International Conference on Robotics for Rehabilitation*, Chicago, IL (2005) pp. 103–108.
4. M. Zinn, O. Khatib, B. Roth and J. K. Salisbury, "Actuation Methods for Human-Centered Robotics and Associated Control Challenges," *2nd Joint CSS/RAS International Workshop on Control Problems in Robotics and Automation*, Las Vegas, NV (Dec. 2002).
5. G. A. Pratt and M. M. Williamson, "Series Elastic Actuators," *IEEE International Conference on Intelligent Robots and Systems*, vol. 1, Pittsburgh, PA (1995) pp. 399–406.
6. G. A. Pratt, M. M. Williamson, P. Dillworth, J. Pratt, K. Ulland and A. Wright, "Stiffness Isn't Everything," *The 4th International Symposium on Experimental Robotics IV*, Stanford, CA, June 30–July 2, (1995) pp. 253–262.
7. D. W. Robinson and J. E. Pratt, "Series Elastic Actuator Development for a Biomimetic Walking Robot," *IEEE/ASME Conference on Advanced Intelligent Mechatronics*, Atlanta, GA (1999) pp. 561–568.
8. C.-M. Chew, G.-S. Hong and W. Zhou, "Series Damper Actuator: A Novel Force/Torque Control Actuator," *4th IEEE/RAS International Conference on Humanoid Robots*, Santa Monica, Los Angeles, CA (2004) pp. 533–546.
9. W. Zhou, C.-M. Chew and G.-S. Hong, "Inverse Dynamics Control for Series Damper Actuator Based on MR Fluid Damper," *IEEE/ASME International Conference on Advanced Intelligent Mechatronics*, Monterey, CA (2005) pp. 473–478.
10. C.-M. Chew, G.-S. Hong and W. Zhou, "Damper System," US Patent. Application No.: 10/845,787 (2004).
11. R. C. Dorf and R. H. Bishop, *Modern Control Systems*, (CRC Press, Boca Roton, FL, 2005).
12. C. W. de Silva, "Sensory information acquisition for monitoring and control of intelligent mechatronic system," *Int. J. Inf. Acquis.* **1**(1), 89–99 (2004).
13. S. Behbahani and C. W. de Silva, "Mechatronic modeling and design," in the book *Mechatronic Systems: Devices, Design, Control, Operation, and Monitoring* (CRC Press, Taylor & Francis, Boca Raton, FL, 2007).
14. X.-J. Lu, C. W. de Silva, M. H. Ang Jr., A.-N. Poo and H. Corporaal, "A New Approach for Mechatronic System Design: Mechatronic Design Quotient," *International Conference on Advanced Intelligent Mechatronics*, Monterey, CA (2005) pp. 911–915.

Appendix A: Proof of the Statement 1

Statement 1: To ensure a minimum overall bandwidth $\omega_{\min}$ for the SDA plant, the damper bandwidth ω_D should satisfy the following requirement:

$$\omega_D \geq \frac{1}{0.64}\omega_{\min}.$$

Proof: The model of the SDA plant and its block diagram are shown in Fig. A1. In the SDA plant, a DC motor (assuming armature control) is connected in series with a damper. The motor's input and output are the armature voltage u and the motor velocity v_m, respectively. Assume that the load end is fixed, the damper's input and output are the motor velocity v_m and the damping force f, respectively. $G_m(s)$, $G_D(s)$, and $G_s(s)$ are the transfer functions of the motor, damper, and SDA plant, respectively.

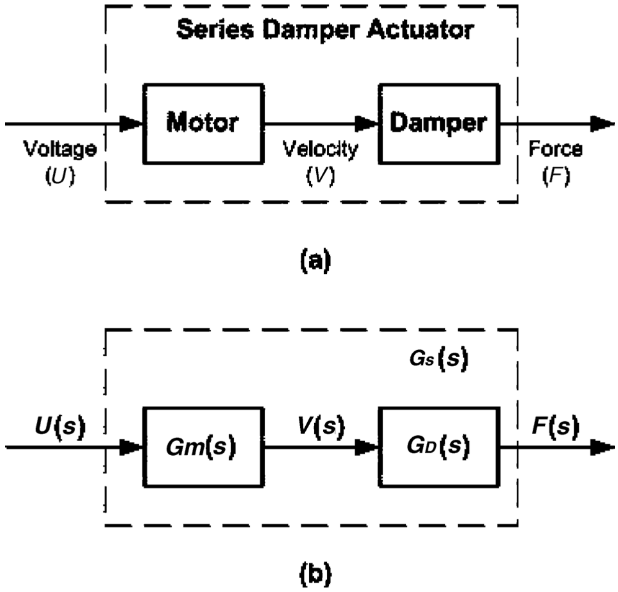

Fig. A1. (a) SDA plant model and (b) the block diagram of the SDA plant.

The transfer function of the DC motor (armature control) $G_m(s)$ can be represented by a first-order model.[11] And as mentioned in Section 3, the transfer function of the damper can also be expressed by a first-order model.[9]
That is

$$G_m(s) = K_m \frac{\omega_m}{s + \omega_m}, \qquad \text{(A 1)}$$

$$G_D(s) = B\frac{\omega_D}{s + \omega_D} \qquad \text{(A 2)}$$

where K_m is the gain of the motor, ω_m is the bandwidth of the motor, B is the gain of the damper, and ω_D is the bandwidth of the damper.

Therefore, the transfer function of the SDA plant can be written as

$$G_s(s) = G_m(s) \cdot G_D(s) = K_m \cdot B\frac{\omega_m\omega_D}{s^2 + (\omega_m + \omega_D)s + \omega_m\omega_D}. \qquad \text{(A 3)}$$

Let ω_s denote the bandwidth of the SDA plant. It can be observed from Eq. (A 3) that, ω_s is fully determined by ω_m and ω_D. Now let us discuss the relationship between ω_s, ω_m, and ω_D.

Assume that

$$\omega_1 = \max\{\omega_m, \omega_D\}, \qquad \text{(A 4)}$$

$$\omega_2 = \min\{\omega_m, \omega_D\}. \qquad \text{(A 5)}$$

Then Eq. (A 3) can be rewritten as

$$G_s(s) = K_m B\frac{\omega_1\omega_2}{s^2 + (\omega_1 + \omega_2)s + \omega_1\omega_2}. \qquad \text{(A 6)}$$

https://doi.org/10.1017/S0263574708004797 Published online by Cambridge University Press

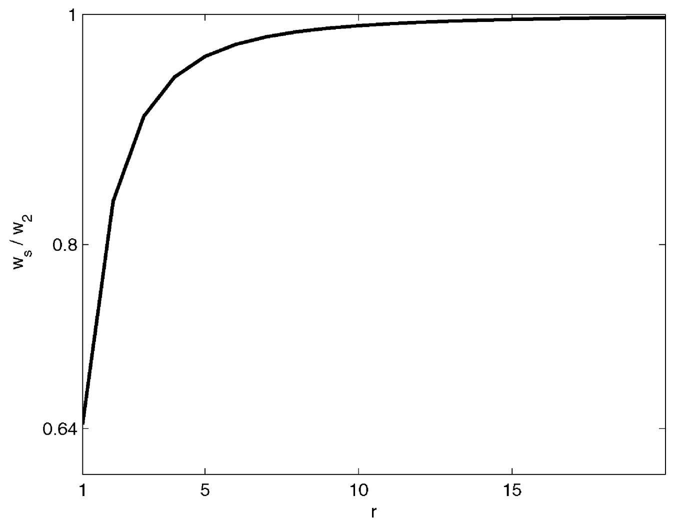

Fig. A2. Bandwidth of SDA plant (G_s) with different values of r.

Normalizing Eq. (A 6) by ω_2^2 yields

$$G_s(S) = K_m B \frac{\omega_1/\omega_2}{(s/\omega_2)^2 + (1 + \omega_1/\omega_2)(s/\omega_2) + \omega_1/\omega_2}$$
$$= K_m B \frac{r}{S^2 + (1 + r)S + r} \quad \text{(A 7)}$$

where $S = s/\omega_2$, $r = \omega_1/\omega_2 \geq 1$.

Based on the definition of the half-power bandwidth, the bandwidth of the SDA plant, ω_s, can be calculated from the following equation:

$$\frac{|G_s(j\omega_s)|}{K_m B} = \frac{1}{\sqrt{2}}. \quad \text{(A 8)}$$

Solving Eq. (A 8) gives

$$\omega_s = \omega_2 \sqrt{\frac{\sqrt{(r^2+1)^2 + 4r^2} - (r^2+1)}{2}}. \quad \text{(A 9)}$$

When $r = 1$

$$\omega_s = \omega_2 \sqrt{\sqrt{2} - 1} = 0.64\omega_2. \quad \text{(A 10)}$$

The plot of ω_s/ω_2 versus r is as shown in Fig. A2. The plot of the gain of $G_s(S)$ [Eq. (A 7)] with different values of r are as shown in Fig. A3. It can be seen from Fig. A2 that as r increases, ω_s approaches ω_2. If $r \gg 1$, that is $\omega_1 \gg \omega_2$, then $\omega_s = \omega_2$. With the decrease in r, the ratio of ω_s over ω_2 will also decrease. The minimum value for ω_s is $0.64\omega_2$ when $r = 1$ or $\omega_1 = \omega_2$. Same results can also be observed from Fig. A3 which contains bode gain plots of $G_s(S)$ with different values of r. From the plot, the bandwidth of $G_s(S)$ (the frequency where the gain drops to $-3\,dB$) is observed to increase from $0.64\omega_2$ to ω_2 with the increase in r.

Now, it can be concluded that the bandwidth of the SDA plant ω_s varies with r from 100% to 64% of ω_2 where ω_2 is the smaller value between the motor bandwidth ω_m and damper bandwidth ω_D. Therefore, if the bandwidth of the motor and the damper are both larger than $\frac{1}{0.64}\omega_{min}$, the overall bandwidth of the SDA system ω_s must be larger than ω_{min}. Therefore, the sufficient condition for $\omega_s \geq \omega_{min}$ is

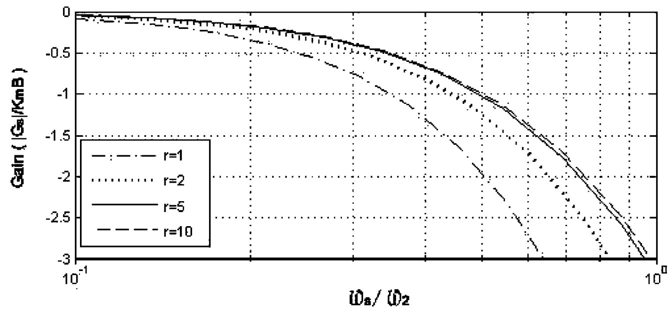

Fig. A3. Gain of SDA plant (G_s) with different values of r.

$$\omega_m \geq \frac{1}{0.64}\omega_{min} \quad \text{and} \quad \omega_D \geq \frac{1}{0.64}\omega_{min}.$$

Hence, Statement 1 is proved.

Appendix B: Proof of Statement 2

Statement 2: To ensure a minimum overall bandwidth ω_{min} for the SDA plant, the DC motor (free end) bandwidth $\omega_{m'}$ should satisfy the following requirement:

$$\omega_{m'} \geq \frac{J_m + J_D/N^2}{0.64 J_m}\omega_{min}.$$

Proof: The DC motor (armature control) transfer function can be written as [11]

$$G_m(s) = \frac{V_m(s)}{U(s)} = \frac{\frac{k_t}{R_a J}}{s + \frac{k_e k_t + R_a b}{R_a J}} = K_m \frac{\omega_m}{s + \omega_m} \quad \text{(B 1)}$$

where b is the equivalent viscous coefficient reflected at the motor shaft, J is the equivalent inertia reflected at the motor shaft, $\omega_m = \frac{k_e\ k_t + R_a\ b}{R_a\ J}$ is the motor bandwidth.

In the SDA plant, the motor shaft is connected to the damper input end via a gear reduction as shown in Fig. B1, where b_m is the rotor damping coefficient of the motor, J_m is the rotor inertia, N is the gear ratio, J_D is the series damper input shaft inertia, and B ($B \geq 0$) is the damping coefficient of the series damper.

We have

$$b = b_m + B/N^2 \quad \text{(B 2)}$$
$$J = J_m + J_D/N^2. \quad \text{(B 3)}$$

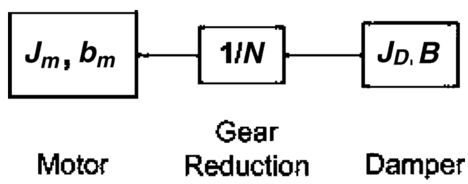

Fig. B1. Motor connected with damper via a gear reduction of ratio N.

https://doi.org/10.1017/S0263574708004797 Published online by Cambridge University Press

When the motor output end is free (without the connection with the series damper), the motor bandwidth $\omega_{m'}$ can be written as

$$\omega_{m'} = \frac{k_e k_t + R_a b_m}{R_a J_m}. \tag{B 4}$$

Since $B \geq 0$, it can be written that

$$\frac{\omega_m}{\omega_{m'}} = \frac{\frac{k_e k_t + R_a b}{R_a J}}{\frac{k_e k_t + R_a b_m}{R_a J_m}} \geq \frac{\frac{k_e k_t + R_a b_m}{R_a J}}{\frac{k_e k_t + R_a b_m}{R_a J_m}} = \frac{J_m}{J} = \frac{J_m}{J_m + J_D/N^2}. \tag{B 5}$$

Therefore,

$$\omega_m \geq \frac{J_m}{J_m + J_D/N^2}\omega_{m'}. \tag{B 6}$$

According to the conclusion made in Appendix A, the motor bandwidth ω_m should satisfy

$$\omega_m \geq \frac{1}{0.64}\omega_{min}. \tag{B 7}$$

Therefore, combining Eq. (B 6), the sufficient condition for Eq. (B 7) is

$$\omega_{m'} \geq \frac{J_m + J_D/N^2}{0.64 J_m}\omega_{min}. \tag{B 8}$$

Hence, Statement 2 is proved.

https://doi.org/10.1017/S0263574708004797 Published online by Cambridge University Press